Proc. Natl. Acad. Sci. USA
Vol. 91, pp. 5672–5676, June 1994
Biochemistry

Cisplatin–DNA adducts are molecular decoys for the ribosomal RNA transcription factor hUBF (human upstream binding factor)

[high-mobility group box/*cis*-diamminedichloroplatinum(II)/anticancer drugs]

DANIEL K. TREIBER*, XIAOQUAN ZHAI*, HANS-MICHAEL JANTZEN†‡, AND JOHN M. ESSIGMANN*§

*Department of Chemistry and Division of Toxicology, Massachusetts Institute of Technology, Cambridge, MA 02139; and †Howard Hughes Medical Institute, Department of Molecular and Cell Biology, University of California at Berkeley, Berkeley, CA 94720

Communicated by Stephen J. Lippard, February 23, 1994 (received for review January 18, 1994)

ABSTRACT **The toxicity of DNA-damaging agents is widely believed to result from the formation of lesions that block polymerases or disrupt the integrity of the genome. A mechanism heretofore not addressed is that DNA damage may titrate essential DNA-binding proteins away from their natural sites of action. This report shows that the ribosomal RNA (rRNA) transcription factor hUBF (human upstream binding factor) binds with striking affinity ($K_{d(app)} \approx 60$ pM) to the intrastrand *cis*-$[Pt(NH_3)_2]^{2+}$–d(GpG) crosslink formed by the anticancer drug *cis*-diamminedichloroplatinum(II) (cisplatin). When protein blots of human cell extracts are probed with cisplatin-modified DNA, 97- and 94-kDa proteins are detected, consistent with the known sizes of hUBF species. A similar analysis of blots containing *in vitro* translated hUBF confirmed that the protein binds cisplatin adducts with high specificity. By contrast, DNA adducts of the clinically ineffective trans isomer of cisplatin, *trans*-diamminedichloroplatinum(II), are not recognized by hUBF. DNase I inhibition patterns of hUBF bound to a 100-base-pair DNA fragment containing a centrally located *cis*-$[Pt(NH_3)_2]^{2+}$–d(GpG) crosslink reveal specific protein–DNA interactions in a 14-base-pair region flanking the adduct. The affinity of hUBF for the rRNA promoter is similar ($K_{d(app)} \approx 18$ pM) to that measured for the cisplatin adduct. In addition, we observe that the hUBF-promoter interaction is highly sensitive to the antagonistic effects of cisplatin–DNA adducts. These results suggest that a cisplatin-mediated transcription-factor-hijacking mechanism could disrupt rRNA synthesis, which is stimulated in proliferating cells.**

cis-Diamminedichloroplatinum(II) (cisplatin) is a widely used anticancer drug that is remarkably effective as a cure for testicular tumors (1). Cytotoxicity is believed to be mediated by cisplatin–DNA adducts, which include mainly 1,2-intrastrand d(GpG) (65%) and d(ApG) (25%) crosslinks and also 1,3-d(GpNpG) (6%) intrastrand crosslinks (2). Cisplatin–DNA adducts may exert their effects by inhibiting DNA and RNA synthesis (2) and by inducing programmed cell death (3). Despite this knowledge, an adequate mechanistic rationale for the significant chemotherapeutic efficacy of this drug remains elusive.

Of possible importance to the cytotoxic mechanism of cisplatin is a family of cisplatin adduct-binding proteins (4, 5) that contain high mobility group (HMG) boxes (6–9). The HMG box is an 80-amino acid region that has conserved basic and aromatic residues and is the structural motif of a novel class of DNA-binding proteins (10–12). An unusual feature of the HMG domain is its affinity for noncanonical DNA structures with sharp angles, such as four-way junctions (13). Of interest is the observation that only the adducts of clinically effective platinum anticancer drugs bind HMG box proteins (HMG-BPs) (7, 14). It is believed that DNA duplex bending and unwinding induced by these cisplatin adducts provide the recognition cues for HMG-BPs (6, 7). HMG1 binds selectively to 1,2 intrastrand *cis*-$[Pt(NH_3)_2]^{2+}$–d(GpG) (G^G) and –d(ApG) crosslinks but lacks specificity for -1,3-d(GpNpG) crosslinks, indicating that the HMG box does not bind to all DNA structures bent by platinum coordination (7). The clinically inactive isomer of cisplatin, *trans*-diamminedichloroplatinum(II), forms 1,3- but not 1,2-intrastrand crosslinks; consequently, DNA modified by this compound is not recognized by HMG-BPs (7, 14). In addition to providing a useful system for studying structure-specific DNA recognition, the selective affinity of HMG-BPs for therapeutically effective cisplatin adducts has suggested a possible role for these proteins in the clinical efficacy of the drug.

Most proteins that interact specifically with damaged DNA play a role in DNA repair. By contrast, HMG-BPs appear to function in processes unrelated to repair, such as transcriptional regulation and the maintenance of chromatin structure (11). There is no evidence to suggest that HMG-BPs act to counter the genotoxic effects of cisplatin adducts; indeed, recent data support the opposite view—specifically, that HMG-BPs somehow sensitize cells to the toxic effects of the drug. A yeast gene encoding the HMG-BP IXR1 confers sensitivity to cisplatin as evidenced by the observation that *IXR1* mutants are 2- to 3-fold more resistant to the drug (9). Although the mechanism by which IXR1 sensitizes cells to cisplatin has yet to be elucidated, one hypothesis suggests that IXR1 shields cisplatin adducts from DNA-repair enzymes. This model seems reasonable because the inefficient repair of cisplatin lesions leads to increased toxicity (15).

DNA repair shielding is not the only mechanism to explain how HMG-BPs could mediate the toxicity of cisplatin. A second model, transcription factor hijacking, proposes that adducts could disrupt cellular homeostasis by sequestering HMG-BPs that regulate the expression of critical genes. Here we show that the HMG-BP human upstream binding factor (hUBF), a critical positive regulator of rRNA transcription (10), binds to cisplatin G^G crosslinks and to its cognate rRNA promoter sequence with comparable affinities.

METHODS

Preparation of Radiolabeled DNA Probes. The DNA probe used for Southwestern blotting was a 422-base-pair (bp) *Ava* I restriction fragment excised from M13mp19 replicative

The publication costs of this article were defrayed in part by page charge payment. This article must therefore be hereby marked "*advertisement*" in accordance with 18 U.S.C. §1734 solely to indicate this fact.

Abbreviations: cisplatin, *cis*-diamminedichloroplatinum(II); G^G, intrastrand *cis*-$[Pt(NH_3)_2]^{2+}$–d(GpG) crosslink; Un-100, unmodified 100-bp DNA fragment; G^G-100, Un-100 containing a centrally located G^G; HMG, high mobility group; HMG-BP, high mobility group box protein; UCE, upstream control element; WCE, whole-cell extract; hUBF, human upstream binding factor; SRY, testis-determining factor [product of the sex-determining region on the Y chromosome (*SRY*)].

‡Present address: COR Therapeutics, Inc., South San Francisco, CA 94080.
§To whom reprint requests should be addressed.

form DNA. Platinated probes were prepared by treating the *Ava* I-digested DNA with cisplatin or *trans*-diamminedichloroplatinum(II), and the formal bound-drug/nucleotide ratios (r_b) were determined by using atomic absorption spectroscopy (5).

For footprinting studies, the *Eco*RI–*Bst*EII fragment of pSBr208 containing the −208 to +78 region of the human rRNA gene was either 5′- or 3′-end-labeled on the noncoding strand. In cases where footprinting probes with higher specific activity were required, the noncoding strand was 3′-end-labeled by using the Klenow enzyme in the presence of [α-^{32}P]dATP, [α-^{32}P]dCTP, and [α-^{32}P]dGTP (>6000 Ci/mmol; 1 Ci = 37 GBq).

A 100-bp DNA fragment containing a single, centrally located 1,2-intrastrand *cis*-[Pt(NH$_3$)$_2$]$^{2+}$–d(GpG) crosslink (G^G-100) and the analogous unmodified fragment (Un-100) were used as both competitor DNAs and probes in hUBF footprinting experiments. The sequence of Un-100 is 5′-CAGATCGATGGACTAGCCAGCTGCCTTGATATCACGTCAGTCTCCTTCTGGTCTCTTCTCAGTCGATGATATCGCTCCAGCTGTTGACTACCCGGGTACT-3′, in which the highlighted bases represent the site of platination in G^G-100. These DNA fragments were provided by P. Pil and S. J. Lippard (7). The adduct-containing strand of G^G-100 and the analogous unmodified strand of Un-100 were 5′-end-labeled with [γ-^{32}P]ATP (>6000 Ci/mmol), and the 5′ end of the unadducted strand was removed with *Ava* I to generate the 90-bp footprinting probes.

Immunoblotting (Western Blotting) and Southwestern Blotting Analyses. HeLa whole-cell extracts (WCEs) were prepared by a sonication procedure (16). The 97-kDa hUBF species was synthesized by *in vitro* transcription and translation from the plasmid pTβGUBF1 as described (17). *In vitro* translated hUBF was quantitated by the incorporation of [^{35}S]methionine. Protein samples (75 μg of WCE or 8 ng of hUBF) were resolved on 5–15% gradient SDS/polyacrylamide gels and transferred to nitrocellulose membranes. For Southwestern analysis, the air-dried membranes were processed as reported (14). In the probing step, the labeled DNA was present at $\approx 5 \times 10^4$ cpm/ml, and the nonspecific competitor poly(dI-dC)·poly(dI-dC) was at 5 μg/ml. Values for the formal drug-bound/nucleotide ratio r_b for probes modified by cisplatin and *trans*-diamminedichloroplatinum(II) were 0.043 and 0.052, respectively. During autoradiography, a 0.254-mm-thick copper sheet was used to block ^{35}S emissions selectively from the *in vitro* translated hUBF. For Western analysis, the filter was probed with a 1:250 dilution of human anti-NOR-90 serum (18) (a gift of E. K. L. Chan), and antibody binding was visualized by using a chemiluminescent detection system (Bio-Rad).

DNase I Footprinting Assays. Homogeneous HeLa hUBF was used to generate DNase I footprints in both rRNA promoter and platinated DNA probes. Footprinting was performed essentially as described (19). hUBF was added to footprinting reactions containing the appropriate, labeled DNA probe (10^3–10^4 cpm, 0.7–50 pM, depending on the experiment) and binding buffer (25 mM Tris·HCl, 7.9/14 mM $MgCl_2$/0.5 mM dithiothreitol/10% glycerol/50 mM KCl/0.05% Nonidet P-40/2.5 mM $CaCl_2$) in a total volume of 50 μl. The binding reactions were incubated at 30°C for 10 min and then digested with DNase I (Worthington DPFF grade) for 1 min at 25°C. The DNase I reactions were terminated by adding a solution of 20 mM EDTA, 1% SDS, 0.2 M NaCl, and 50 μg of yeast total RNA per ml. Deproteinized DNA samples were analyzed by electrophoresis through wedged sequencing gels. Gels were fixed, dried, and exposed with an intensifying screen to preflashed x-ray film at −80°C and analyzed by using a Molecular Dynamics PhosphorImager.

RESULTS

hUBF Binds Selectively to Cisplatin-Modified DNA. Protein blots of human HeLa cell extracts (Fig. 1*A*) probed with cisplatin-modified DNA (Southwestern analysis) revealed species of ≈97, 94, and 28 kDa. Unmodified DNA or DNA modified with the clinically ineffective trans-diamminedichloroplatinum(II) compound is not bound by these proteins (Fig. 1 *B* and *C*), although a 105-kDa nonspecific DNA-binding protein was detected with each of the three DNA probes. A current research focus has been to define the natural function of these proteins to elucidate their possible relevance to the mechanism of action of cisplatin. The 28-kDa species has been identified recently as the abundant chromatin protein HMG1 (7, 8). The precise functions of HMG1 remain unclear, although it has been proposed to play roles in the maintenance of chromosome structure and the alteration of DNA topology (20). HMG1 may thereby be important for transcription and DNA replication (20). Since the HMG box is a unifying feature of many cisplatin-damage-recognition proteins, it was reasoned that the 97- and 94-kDa species may possess this DNA-binding domain. The RNA polymerase I transcription factor hUBF contains several regions of homology to HMG1 (10) and exists as both 97- and 94-kDa species because of an alternative splicing event (18). A Western blot probed with hUBF antiserum shows that the hUBF doublet resembles the bands detected by Southwestern analysis (compare Fig. 1 *A* and *D*). These observations led to the hypothesis that hUBF binds to cisplatin-modified DNA. Southwestern analysis of *in vitro* translated hUBF confirmed this notion (Fig. 1*A*, lane 2).

hUBF Makes Specific DNA Contacts in the Region Flanking an Intrastrand G^G Crosslink. The specificity of the interaction between cisplatin adducts and hUBF was examined by DNase I footprinting (Fig. 2). hUBF was added to a 100-bp double-stranded DNA fragment containing a single cisplatin–G^G adduct (G^G-100). A distinct protection pattern was observed in the 14-bp region encompassing the adduct (Fig. 2*A*, lane 1) providing direct evidence that hUBF recognizes the structural distortion induced by G^G. The established structural features of this adduct include helix bending (34°) toward the major groove (21) and unwinding (−13°) (22). No such protection is afforded the analogous unmodified 100-mer (Fig. 2*A*, lane 3). The cisplatin lesion is centered within the protected region. The phosphodiester bond immediately 5′ to the adduct remains sensitive to DNase I.

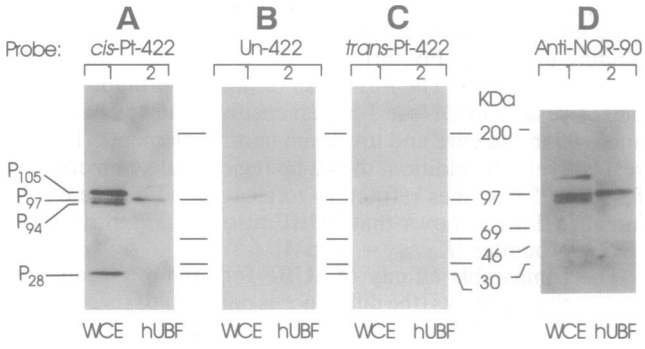

FIG. 1. hUBF binds selectively to cisplatin-modified DNA. Parallel blots of HeLa WCE and *in vitro* translated hUBF were probed with various ^{32}P-labeled DNA fragments in Southwestern analyses (*A–C*) or with antiserum against hUBF (anti-NOR-90) (*D*). The DNA probes were modified by either cisplatin (*cis*-Pt-422) (*A*) or trans-diamminedichloroplatinum(II) (trans-Pt-422) (*C*). In *B*, the blot was probed with unmodified DNA (Un-422). HeLa proteins recognizing cis-Pt-422 are listed by molecular mass in kDa to the left of *A*. The positions of both HeLa and *in vitro* translated hUBF are shown in the Western blot (*D*). A 120-kDa species of unknown identity is also visualized in the WCE with anti-NOR-90.

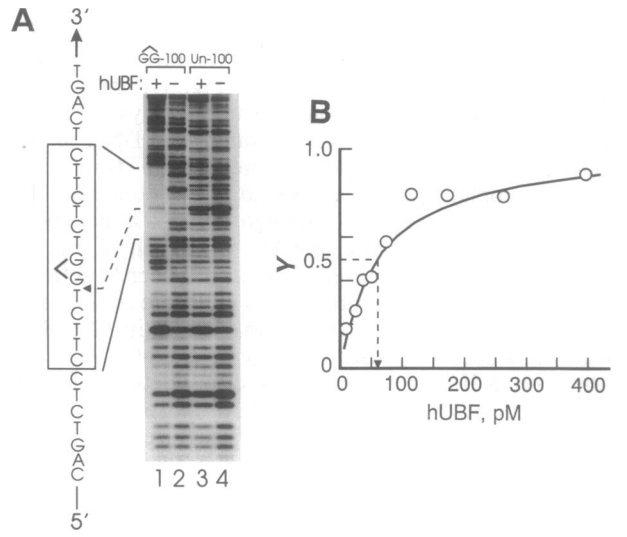

FIG. 2. DNase I footprint analysis of [hUBF–GˆG-100] complexes. (*A*) GˆG-100 is protected from DNase I cleavage in the presence of 400 pM hUBF (compare lanes 1 and 2). The relevant sequence is shown to the left, and the protected residues are displayed within the box. The broken line indicates a residue immediately 5′ to GˆG that remains DNase I-sensitive. The control fragment, Un-100, gives the same cleavage pattern both in the presence and in the absence of hUBF (lanes 3 and 4). Note that the cleavage patterns of GˆG-100 and Un-100 are different near the cisplatin adduct (lanes 2 and 4). (*B*) The DNase I protection assay was used to characterize hUBF binding to GˆG-100. *Y* is the fractional saturation of GˆG-100 and was estimated by monitoring the intensity of three bands in the protected region at hUBF concentrations ranging from 6 to 400 pM. The data fit the equation K_d = [hUBF][GˆG-100]/[hUBF–GˆG-100] when K_d = 60 pM. The protein concentration giving half-maximal binding ($K_{d(app)}$) is indicated by the broken line. The labeled probe was present at 20 pM (10^4 cpm).

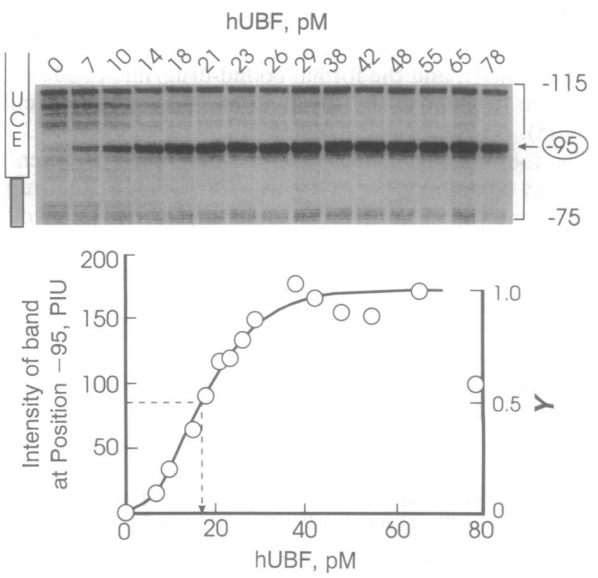

FIG. 3. Binding isotherm describing hUBF–rRNA promoter interactions. (*Upper*) Promoter binding at hUBF concentrations ranging from 7 to 78 pM is shown and is most easily visualized by the increased DNase I sensitivity of the −95 position in the UCE. The 3′-labeled probe in this assay was present at 0.7 pM (10^3 cpm). The bands appear as doublets because of incomplete labeling. (*Lower*) hUBF binding in *Upper* was quantitated by measuring the intensity of the enhanced cleavage at −95. Binding is reported to the left in arbitrary PhosphorImager units (PIU); data to the right are expressed as the apparent fractional saturation (*Y*). The protein concentration giving half-maximal binding ($K_{d(app)}$) is indicated by the broken line. A Hill plot of these data yielded a best-fit line (r = 0.997) with a Hill constant (n_H) of 2.7, indicating positive cooperativity.

hUBF Binds to Cisplatin Adducts and rRNA Promoter Sequences with Comparable Affinities. The biological significance of adduct recognition by hUBF ultimately depends on the affinity of the interaction. The interaction of hUBF with rDNA provides a useful benchmark value for a biologically relevant affinity. Accordingly, the affinity of hUBF for both cisplatin adducts and rDNA sequences was measured. The formation of [hUBF–GˆG-100] complexes was exceptionally favorable. Quantitative DNase I protection assays estimated the apparent dissociation constant ($K_{d(app)}$) to be 60 pM (Fig. 2*B*), and the data were consistent with a noncooperative binding modality. Footprinting was also used to quantitate promoter binding. The formation of [hUBF–promoter] complexes results in DNase I hypersensitivity at positions −20 and −95 in the core and upstream control elements (UCEs), respectively. In addition, the 40-bp region that symmetrically flanks −95 becomes refractory to cleavage (19). The experiment in Fig. 3 shows that hUBF also binds tightly to the rRNA promoter [$K_{d(app)}$ = 18 pM].

The comparable affinity of hUBF for promoter sequences and cisplatin adducts (the difference is only 3-fold) suggests that adducts may act as molecular decoys for hUBF in a cellular milieu. Of possible importance to this comparison, however, is the observation that promoter-bound hUBF interacts with a second factor, the TATA-binding protein complex hSL1 (17). Cooperative interactions with hSL1 may further increase the affinity of the hUBF–promoter interaction, and the 3-fold specificity factor should be viewed as a lower limit.

The hUBF–promoter binding isotherm reveals that the fraction of bound promoter (*Y*) increases sharply over a narrow range of hUBF concentrations, suggesting that binding is cooperative (Hill constant, n_H = 2.7) (Fig. 3). Cooperativity has been observed previously for *Xenopus* UBF binding to enhancer repeats (23). An important consequence of cooperativity in the context of the transcription-factor-hijacking model is that small changes in the pool of free hUBF can strongly alter promoter occupancy.

Cisplatin Adducts Inhibit the Formation of [hUBF–rRNA Promoter] Complexes. The affinity constants presented above suggest that cisplatin adducts should be effective competitive inhibitors of [hUBF–promoter] complex formation. This view is supported by Fig. 4, which shows that GˆG-100 efficiently antagonized hUBF–promoter interactions. The reduced intensity of bands at positions −21 and −95 in the core and UCE elements and the reappearance of bands between positions −75 and −115 illustrate this effect (Fig. 4, lanes 7–12). At a saturating concentration of hUBF, the formation of promoter complexes was completely inhibited by a platinum adduct concentration of 5 nM (lane 11), which is well below the adduct levels in cancer patient DNA (10^4–10^5 complexes per cell, or 0.1–1 μM) (24). The corresponding unmodified competitor DNA (Un-100) was a weaker competitor of hUBF than GˆG-100 (Fig. 4, lanes 3–6) by a factor of 10–30. Since Un-100 contains up to 100 overlapping nonspecific binding sites compared with the one specific binding site in GˆG-100, the preference of hUBF for a platinated over an unplatinated site may be as high as 1–3 × 10^3-fold.

DISCUSSION

We have demonstrated that the nucleolar transcription factor hUBF binds with high affinity and specificity to the major DNA adduct of the anticancer drug cisplatin. hUBF is the first example of a HMG-BP of known function that binds selectively to cisplatin DNA adducts. The affinity of hUBF for GˆG was substantial [$K_{d(app)}$ = 60 pM]. For comparison, the [HMG1–GˆG-100] complex has a $K_{d(app)}$ of 370 nM (7). hUBF (this work) and HMG1 (7) display a similar preference for a platinated site over an unplatinated site, suggesting that

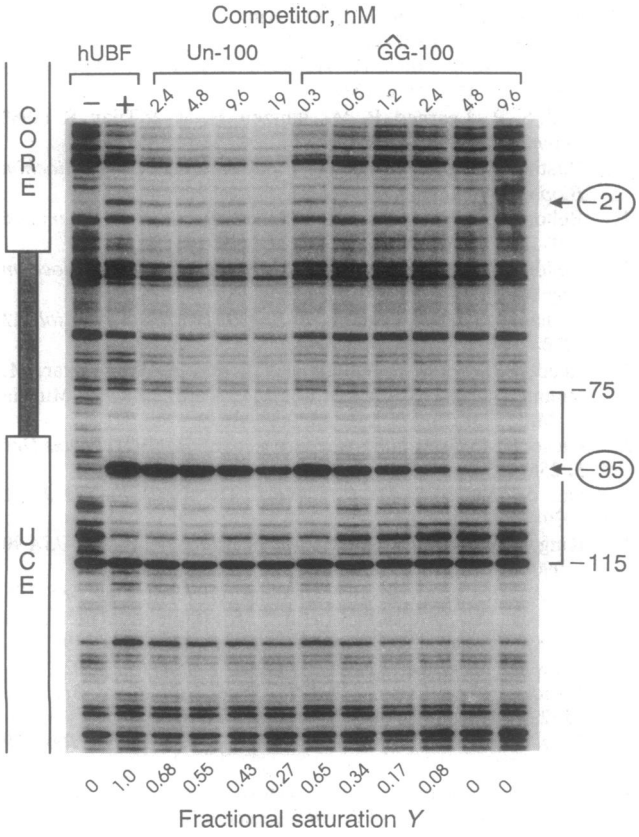

FIG. 4. hUBF–rRNA promoter interactions are antagonized by cisplatin–DNA adducts. The ability of G^G-100 to compete with rRNA sequences for hUBF binding is evaluated. Promoter binding is visualized by DNase I footprinting as in Fig. 3 except that the enhanced cleavage at −21 in the core is also shown. Purified HeLa hUBF was added to all samples except the negative control (lane 1) to a final concentration of 160 pM. This level of hUBF is safely above that producing an apparent fractional saturation (Y) of 1 in the positive control (lane 2). The 5′-labeled probe was present at 46 pM (10^4 cpm). Un-100 (lanes 3–6) and G^G-100 (lanes 7–12) were added as unlabeled competitors to the final nanomolar concentrations listed. The competitive effect was estimated by measuring Y of the promoter probe. Y values are shown at the bottom. Lanes 1 and 2 were used as standards to calculate Y in lanes 3–12.

the higher absolute affinity measured for hUBF may stem from nonspecific DNA contacts made by the additional HMG box domains. The significant nonspecific binding component for hUBF (Fig. 4) is also observed with other HMG-BPs, including lymphoid enhancer factor 1 (LEF-1), which binds with nominal specificity (20- to 40-fold) to its putative recognition sequence (25).

Our data lend insight into the structural features of [hUBF–G^G-100] complexes. The adduct was approximately centered within the 14-bp protected region, suggesting that the DNA-binding domain(s) is symmetrically placed relative to the adduct. The elbow of the adduct-induced DNA bend appears to be solvent exposed, however, because the phosphodiester bond immediately 5′ to the lesion remained sensitive to DNase I. Precedent suggests that the interaction is likely to occur in the minor groove, on the convex side of the DNA bend; lymphoid enhancer factor 1 and SRY [the testis-determining factor encoded by the sex-determining region on the Y chromosome (*SRY*)] bind to their putative recognition sequences through minor groove interactions (25–27).

hUBF, like SRY, exhibits both sequence-specific and structure-specific modes of DNA recognition. The footprinting data suggest that the structure-specific [hUBF–G^G-100] and sequence-specific [hUBF–UCE] complexes share structural homologies; in each case a protected region symmetrically flanks a nuclease-sensitive site. DNA bending is the likely common feature of these complexes. Indeed, a hallmark of the HMG domain is its propensity to interact with bent DNA and also to induce bending in linear sequences. SRY, to give one example, efficiently recognizes four-way DNA junctions with sharp angles (13). Furthermore, SRY induces a sharp bend (85°) in a specific DNA sequence upon binding (28). The specific interactions of the HMG domain with bent DNAs may be attributed to its "L"-shaped cleft, as reported recently (29). hUBF probably also bends DNA, although detailed structural studies have yet to be performed. The DNase I-hypersensitive site induced in the UCE upon hUBF binding may indicate DNA bending because DNase I activity is sensitive to structural features of DNA, including the width of the minor groove (30). The putative bend site is centered within a UCE region that is protected from DNase I; interestingly, the G^G-induced DNA bend is also centered within a DNase I-resistant region. These observations suggest that the bent and unwound DNA structure induced by G^G may mimic a favorable DNA conformation that occurs during the formation of a stable [hUBF–promoter] complex. A similar model was proposed recently to explain structure-specific recognition by SRY (27). With hUBF, we suggest that the bent and unwound structure of the DNA adduct overcomes the requirement for a sequence-specific recognition element.

hUBF binds to rRNA promoter sequences and cisplatin adducts with comparable affinities, leading to the hypothesis that adducts can act as effective decoys for hUBF binding (Figs. 2 and 3), a view that is supported by the *in vitro* competition assays (Fig. 4). What effects could adduct recognition by hUBF have on normal cellular processes? We propose that both DNA repair and rRNA transcription would be negatively affected. Importantly, both processes are probably more critical for proliferating cells, such as tumor cells, than for stationary cells (31, 32). Since the cellular levels of hUBF and cisplatin lesions are similar ($\approx 5 \times 10^4$ lesions per cell) (19, 24), biologically significant adverse effects on both transcription and repair are predicted.

hUBF binding may impede the removal of cisplatin adducts by DNA repair enzymes. Although it is clear that G^G adducts are excised in human cells (33), recent studies with cellular extracts suggest that the repair may be inefficient (34). Our data show that the 14-bp region flanking the G^G lesion is strongly protected from nuclease cleavage. It is reasonable to speculate that this region would also be shielded from components of the mammalian DNA repair machinery. In support of this argument, the XPAC (xeroderma pigmentosum complementation group A correcting) protein, which recognizes damaged DNA and is essential for human nucleotide excision repair, has a relatively low affinity for G^G lesions [$K_{d(app)} > 600$ nM] (35). XPAC would not be expected to displace hUBF, which binds adducts much more tightly.

Hijacking of hUBF by G^G adducts may also adversely affect cellular welfare by disrupting the regulation of rRNA synthesis. In cisplatin-treated cells, the formation of high-affinity binding sites for hUBF could reduce the amount of hUBF available for promoter binding. The ultimate effect on rRNA synthesis could be significant because of the steep relationship between promoter occupancy and the ambient hUBF concentration (Fig. 3).

Finally, our results have implications for novel drug design. Conventional transcription factor decoys of therapeutic potential typically consist of short oligonucleotides containing appropriate recognition sequences (36, 37). The results presented here suggest that small molecules, such as cisplatin, that alter DNA structure can thereby function as molecular decoys for transcription factors. Small molecules may

provide the benefits of molecular hijacking agents without the anticipated drug delivery problems of therapeutic oligonucleotides.

D.K.T. and X.Z. contributed equally to these studies. We thank R. Tjian for his support of this work. We also thank S. J. Lippard and J. R. Williamson for comments on the manuscript, P. Pil and S. J. Lippard for G^G-100, E. Chan for anti-NOR-90, and A. Barrasso for technical assistance. This study was supported by National Institutes of Health Grants CA52127 and ES07020.

1. Loehrer, S. J. & Einhorn, L. H. (1984) *Ann. Int. Med.* **100,** 704–713.
2. Bruhn, S. L., Toney, J. H. & Lippard, S. J. (1990) *Prog. Inorg. Chem.* **38,** 477–516.
3. Eastman, A. (1993) *Cancer Cells* **5,** 275–280.
4. Chu, G. & Chang, E. (1988) *Science* **242,** 564–567.
5. Donahue, B. A., Augot, M., Bellon, S. F., Treiber, D. K., Toney, J. H., Lippard, S. J. & Essigmann, J. M. (1990) *Biochemistry* **29,** 5872–5880.
6. Bruhn, S. L., Pil, P. M., Essigmann, J. M., Housman, D. E. & Lippard, S. J. (1992) *Proc. Natl. Acad. Sci. USA* **89,** 2307–2311.
7. Pil, P. M. & Lippard, S. J. (1992) *Science* **256,** 234–237.
8. Hughes, E. N., Engelsberg, B. N. & Billings, P. C. (1992) *J. Biol. Chem.* **267,** 13520–13527.
9. Brown, S. J., Kellett, P. J. & Lippard, S. J. (1993) *Science* **261,** 603–605.
10. Jantzen, H.-M., Admon, A., Bell, S. P. & Tjian, R. (1990) *Nature (London)* **344,** 830–836.
11. Lilley, D. M. J. (1992) *Nature (London)* **357,** 282–283.
12. Bianchi, M. E., Falciola, L., Ferrari, S. & Lilley, D. M. J. (1992) *EMBO J.* **11,** 1055–1063.
13. Ferrari, S., Harley, V. R., Pontiggia, A., Goodfellow, P. N., Lovell-Badge, R. & Bianchi, M. E. (1992) *EMBO J.* **11,** 4497–4506.
14. Toney, J. H., Donahue, B. A., Kellett, P. J., Bruhn, S. L., Essigmann, J. M. & Lippard, S. J. (1989) *Proc. Natl. Acad. Sci. USA* **86,** 8328–8332.
15. Fraval, H. N. A., Rawlings, C. J. & Roberts, J. J. (1978) *Mutation Res.* **51,** 121–132.
16. Samson, L., Derfler, B. & Waldstein, E. A. (1986) *Proc. Natl. Acad. Sci. USA* **83,** 5607–5610.
17. Jantzen, H.-M., Chow, A. M., King, D. S. & Tjian, R. (1992) *Genes Dev.* **6,** 1950–1963.
18. Chan, E. K. L., Imai, H., Hamel, J. C. & Tan, E. M. (1991) *J. Exp. Med.* **174,** 1239–1244.
19. Bell, S. P., Learned, R. M., Jantzen, H.-M. & Tjian, R. (1988) *Science* **241,** 1192–1197.
20. Bustin, M., Lehn, D. A. & Landsman, D. (1990) *Biochim. Biophys. Acta* **1049,** 231–243.
21. Bellon, S. F. & Lippard, S. J. (1990) *Biophys. Chem.* **35,** 179–188.
22. Bellon, S. F., Coleman, J. H. & Lippard, S. J. (1991) *Biochemistry* **30,** 8026–8035.
23. Putnam, C. D. & Pikaard, C. S. (1992) *Mol. Cell. Biol.* **12,** 4970–4980.
24. Reed, E., Parker, R. J., Gill, I., Bicher, A., Dabholkar, M., Vionnet, J. A., Bostick-Bruton, F., Tarone, R. & Muggia, F. M. (1993) *Cancer Res.* **53,** 3694–3699.
25. Giese, K., Amsterdam, A. & Grosschedl, R. (1991) *Genes Dev.* **5,** 2567–2578.
26. van de Wetering, M. & Clevers, H. (1992) *EMBO J.* **11,** 3039–3044.
27. King, C. & Weiss, M. A. (1993) *Proc. Natl. Acad. Sci. USA* **90,** 11990–11994.
28. Giese, K., Cox, J. & Grosschedl, R. (1992) *Cell* **69,** 185–195.
29. Weir, H. M., Kraulis, P. J., Hill, C. S., Raine, A. R. C., Laue, E. D. & Thomas, J. O. (1993) *EMBO J.* **12,** 1311–1319.
30. Drew, H. R. & Travers, A. A. (1984) *Cell* **37,** 491–502.
31. Mauck, J. C. & Green, H. (1973) *Proc. Natl. Acad. Sci. USA* **70,** 2819–2822.
32. Fraval, H. N. A. & Roberts, J. J. (1979) *Cancer Res.* **39,** 1793–1797.
33. Fichtinger-Schepman, A. M., van Oosterom, A. T., Lohman, P. H. M. & Berends, F. (1987) *Cancer Res.* **47,** 3000–3004.
34. Szymkowski, D. E., Yarema, K., Essigmann, J. M., Lippard, S. J. & Wood, R. D. (1992) *Proc. Natl. Acad. Sci. USA* **89,** 10772–10776.
35. Jones, C. J. & Wood, R. D. (1993) *Biochemistry* **32,** 12096–12104.
36. Bielinska, A., Shivdasani, R. A., Zhang, L. & Nabel, G. J. (1990) *Science* **250,** 997–1000.
37. Chu, B. C. F. & Orgel, L. E. (1992) *Nucleic Acids Res.* **20,** 5857–5858.